Improved Technique for Determining Complex Permittivity with the Transmission/Reflection Method

JAMES BAKER-JARVIS, MEMBER, IEEE, ERIC J. VANZURA, MEMBER, IEEE, AND WILLIAM A. KISSICK, MEMBER, IEEE

Abstract—**The transmission/reflection method for complex permittivity and permeability determination is studied. The special case of permittivity measurement is examined in detail. New robust algorithms for permittivity determination that eliminate the ill-behaved nature of the commonly used procedures at frequencies corresponding to integer multiples of one-half wavelength in the sample are presented. An error analysis is presented which yields estimates of the errors incurred due to the uncertainty in scattering parameters, length measurement, and reference plane position. In addition, new equations are derived for determining complex permittivity independent of reference plane position and sample length.**

I. Introduction

BROAD-BAND measurements of complex permittivity and permeability are required for a multitude of applications. Due to its relative simplicity, the transmission/reflection (TR) method is presently a widely used broad-band measurement technique. The relevant literature in this area is copious and no attempt is made in this paper to review it exhaustively. A measurement using the TR method proceeds by placing a sample in a section of waveguide or coaxial line and measuring the two-port complex scattering parameters, preferably by an automatic network analyzer (ANA). The scattering equations then relate the measured scattering parameters to the permittivity and permeability of the material. The system of equations contains as unknowns the complex permittivity and permeability, the calibration reference plane positions, and, in some applications, the sample length. This system of equations is generally overdetermined and therefore can be solved in various ways. From a pragmatic viewpoint, what is needed are equations that are stable over the frequency range of interest and equations that do not depend on the position of the calibration reference plane.

With the development of modern network analyzer systems there is generally no paucity of data; thus correct and efficient numerical algorithms for the reduction of the scattering data are of paramount importance. To accommodate modern network analyzer acquisition systems, Nicolson and Ross [1] and Weir [2] introduced procedures for obtaining broad-band measurements in both time and frequency domains. In the Nicolson–Ross procedure, the equations for the scattering parameters are combined in such a fashion as to allow the system of equations to decouple, yielding an explicit equation for the permittivity and permeability as a function of the scattering parameters. This solution has formed the basis of the commonly utilized technique for obtaining permittivity and permeability from scattering measurements [3]–[5]. The compact form of these equations, while elegant, is not well behaved for low-loss materials at frequencies corresponding to integer multiples of one-half wavelength in the sample. At these frequencies the solution for low-loss materials is divergent. Many researchers have bypassed this problem by using samples which are less than one-half wavelength long at the highest measurement frequency. However, this approach, as shown later in the paper, severely limits the viability of the TR method since short samples increase measurement uncertainty.

Stuchly and Matuszewski [6] presented a slightly different derivation from that of Nicolson and Ross and obtained two explicit equations for the permittivity. They showed that one of these equations was ambiguous; the other equation was similar to the Nicolson–Ross equation which is unstable for low-loss materials at multiples of one-half integer wavelengths. Ligthardt [7], in a detailed analysis, presented a method for shorted line measurements where the scattering equations for the permittivity were solved over a calculated uncertainty region and the results were then averaged. The equations used by Ligthardt are useful for high-loss materials, but for low-loss materials they suffer the same pathologies as the Nicolson–Ross [1] and Weir [2] equations at multiples of one-half wavelength. It can be shown that the Nicolson–Ross–Weir solution for combined permeability and permittivity for low-loss materials is inherently divergent at integer multiples of one-half wavelength in the sample. In this paper we present a procedure for obtaining complex permittivity from the scattering equations which is stable over the frequency spectrum. This procedure minimizes the instability of the Nicolson–Ross–Weir equations by

Manuscript received November 2, 1989; revised March 30, 1990.
The authors are with the Broadband Microwave Metrology Group, National Institute of Standards and Technology, Boulder, CO 80303.
IEEE Log Number 9036432.

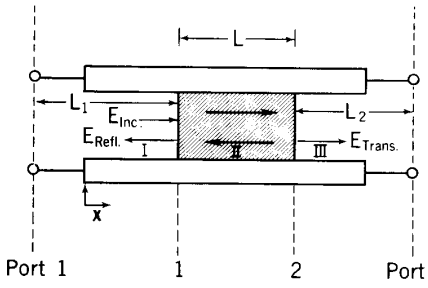

Fig. 1. A dielectric sample in a transmission line and the incident (inc) and reflected (refl) electric field distributions in regions I, II, and III. Port 1 and port 2 denote calibration reference plane positions.

setting $\mu_R^* = 1$. This new procedure allows measurements to be taken on samples of arbitrary length.

Another problem encountered in practice is the transformation of S-parameter measurements from the calibration reference planes to the ends of the sample. This transformation requires knowledge of the position of the sample in the sample holder; however this information may be limited in many applications. The port extension feature of network analyzers is of some help in determining reference plane position, but does not completely solve the problem. Equations that are independent of reference plane positions are desirable. Also, equations that are independent of sample length are useful for high-temperature applications. In the past, other authors addressed the problem of either reference plane invariance or sample length invariance, for example Altschuler [8], Harris [9], and Scott [10], but no one, to our knowledge, has addressed the problem of combined reference plane and sample length invariance.

The goal of this paper is threefold: first, to examine the scattering equations in detail and to present an improved method for solving the transmission line equations in an iterative fashion with application to permittivity measurements; second, to derive scattering equations that are simultaneously invariant to the position of the reference planes and sample length; and, third, to present an uncertainty analysis for this new procedure.

II. Theory

In the TR measurement technique, a sample is inserted into either a waveguide or a coaxial line and the sample is subjected to an incident electromagnetic field (see Fig. 1). The scattering equations are found from an analysis of the electric field at the sample interfaces. If we assume electric fields $E_{\rm I}$, $E_{\rm II}$, and $E_{\rm III}$ (with a time dependence of $\exp(j\omega t)$) in the regions I, II, and III, we can write the spatial distribution of the electric field where the incident electric field is 1:

$$E_{\rm I} = \exp(-\gamma_0 x) + C_1 \exp(\gamma_0 x) \tag{1}$$

$$E_{\rm II} = C_2 \exp(-\gamma x) + C_3 \exp(\gamma x) \tag{2}$$

$$E_{\rm III} = C_4 \exp(-\gamma_0 x) + C_5 \exp(\gamma_0 x) \tag{3}$$

where

$$\gamma = j\sqrt{\frac{\omega^2 \mu_R^* \epsilon_R^*}{c_{\rm vac}^2} - \left(\frac{2\pi}{\lambda_c}\right)^2} \tag{4}$$

$$\gamma_0 = j\sqrt{\left(\frac{\omega}{c_{\rm lab}}\right)^2 - \left(\frac{2\pi}{\lambda_c}\right)^2} \tag{5}$$

$$\epsilon = [\epsilon_R' - j\epsilon_R'']\epsilon_0 = \epsilon_R^* \epsilon_0 \tag{6}$$

$$\mu = [\mu_R' - j\mu_R'']\mu_0 = \mu_R^* \mu_0. \tag{7}$$

Here, $j = \sqrt{-1}$, $c_{\rm vac}$ and $c_{\rm lab}$ are the speed of light in vacuum and in air respectively, ω is the angular frequency, λ_c is the cutoff wavelength, ϵ_0 and μ_0 are the permittivity and permeability of vacuum, ϵ_R^* and μ_R^* are the complex permittivity and permeability relative to a vacuum, and γ_0 and γ are the propagation constants in air and the material respectively. The constants C_i are determined from the boundary conditions. The boundary condition on the electric field is the continuity of the tangential component at the interfaces. The boundary condition on the magnetic field requires the assumption that no surface currents are generated. If this condition holds, then the tangential component of the magnetic field is continuous across the interface. The tangential component of the magnetic field can be calculated from Maxwell's equations.

For a two-port device the expressions for the measured scattering parameters are obtained by solving (1)–(3) subject to the boundary conditions. Since the S matrix is symmetric, $S_{12} = S_{21}$. The explicit expressions are given by

$$S_{11} = R_1^2 \left[\frac{\Gamma(1-z^2)}{1-\Gamma^2 z^2}\right] \tag{8}$$

$$S_{22} = R_2^2 \left[\frac{\Gamma(1-z^2)}{1-\Gamma^2 z^2}\right] \tag{9}$$

$$S_{21} = R_1 R_2 \left[\frac{z(1-\Gamma^2)}{1-\Gamma^2 z^2}\right] \tag{10}$$

where

$$R_1 = \exp(-\gamma_0 L_1) \tag{11}$$

$$R_2 = \exp(-\gamma_0 L_2) \tag{12}$$

where L_1 and L_2 are the distances from the calibration reference planes to the sample ends, and R_1 and R_2 are the reference plane transformation expressions. Of course, (8)–(10) are not new and are derived in detail elsewhere [1], [11]. We define a reflection coefficient by

$$\Gamma = \frac{\dfrac{\gamma_0}{\mu_0} - \dfrac{\gamma}{\mu}}{\dfrac{\gamma_0}{\mu_0} + \dfrac{\gamma}{\mu}} \tag{13}$$

and for coaxial line ($\omega_c \to 0$) the reflection coefficient

reduces to

$$\Gamma = \frac{\frac{c_{vac}}{c_{lab}}\sqrt{\frac{\mu_R^*}{\epsilon_R^*}} - 1}{\frac{c_{vac}}{c_{lab}}\sqrt{\frac{\mu_R^*}{\epsilon_R^*}} + 1}. \tag{14}$$

We also have an expression for z, the transmission coefficient:

$$z = \exp(-\gamma L) \tag{15}$$

where L is the sample length. We assume that we know the total length of the sample holder: $L_{air} = L + L_1 + L_2$. Additionally, S_{21} for the empty sample holder is

$$S_{21}^0 = R_1 R_2 \exp(-\gamma_0 L). \tag{16}$$

For nonmagnetic materials, (8), (9), and (10) contain ϵ_R', ϵ_R'', L, and the reference plane transformations R_1 and R_2 as unknown quantities. Since the equations for S_{12} and S_{21} are equivalent for isotropic materials, we have four complex equations, (8), (9), (10), and (16), plus the equation for the length of the air line or equivalently, nine real equations for the five unknowns. Additionally, in many applications we know the sample length. For magnetic materials we have seven unknowns. Thus, the system of equations is overdetermined and it is possible to solve the equations in various combinations. As an example, in nonmagnetic materials if the position of the reference planes is not known accurately, then L_1 and L_2 can be eliminated from the equations to obtain equations that are reference-plane invariant. There exists a whole family of reference-plane independent equations and only the most useful are given below as examples:

$$|S_{21}| = \left|\frac{z(1-\Gamma^2)}{1-z^2\Gamma^2}\right| \tag{17}$$

$$|S_{11}| = \left|\frac{\Gamma(1-z^2)}{1-z^2\Gamma^2}\right| \tag{18}$$

$$\frac{S_{11}S_{22}}{S_{12}S_{21}} = \frac{\left(1-\frac{\epsilon_R^*}{\mu_R^*}\right)^2}{\frac{4\epsilon_R^*}{\mu_R^*}} \sinh^2 \gamma L \tag{19}$$

$$\frac{S_{21}}{S_{21}^0} = \exp(\gamma_0 L)\frac{z[1-\Gamma^2]}{1-z^2\Gamma^2} \tag{20}$$

$$S_{21}S_{12} - S_{11}S_{22} = \exp[(-2\gamma_0)(L_{air} - L)]\frac{z^2-\Gamma^2}{1-z^2\Gamma^2}. \tag{21}$$

Here the vertical bar denotes the magnitude of the complex expression. Equation (19) is valid only for coaxial line. Equation (21) is the determinant of the scattering matrix; the determinant is well known as a quantity invariant to rotations.

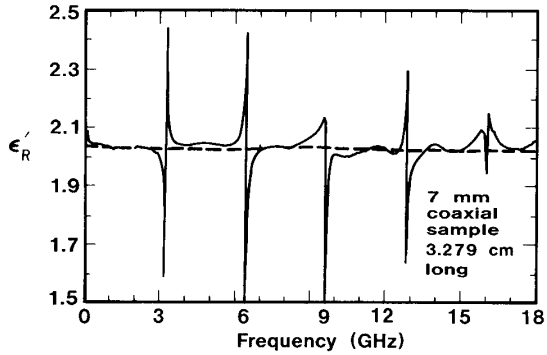

Fig. 2. The determination of the permittivity of a PTFE sample as a function of frequency using the Nicolson and Ross equations (solid line) and the iteration procedure (dashed line) (eq. (21)).

Nicolson and Ross [1] and also Weir [2] combined the equations for S_{11} and S_{21}, (8) and (10), and discovered an explicit formula for the permittivity and permeability. The solution of these equations, however, is not totally straightforward in that an ambiguity in phase must be resolved at each frequency by matching calculated and measured group delay. Also, this procedure does not work well at frequencies where the sample length is a multiple of one-half wavelength in the material. Typical results calculated from the Nicolson–Ross–Weir [1], [2] equations are displayed in Fig. 2 as the solid line. At frequencies corresponding to integer multiples of one-half wavelength in low-loss materials the scattering parameter $|S_{11}|$ gets very small. The equations are algebraically unstable as $S_{11} \to 0$; also for small $|S_{11}|$, the ANA phase uncertainty is large. Since the solution is proportional to $\left(\frac{1}{S_{11}}\right)$ we see that the phase error dominates the solution at these frequencies. To bypass this problem, many researchers resort to using short samples. However, use of short samples lowers the measurement sensitivity. In fact, as will be shown in Section III, to minimize the uncertainty in low-loss materials a relatively long sample is preferred.

Iterative solution of various combinations of (17)–(21) produces a solution that is stable over the measurement spectrum. Sample length and air line length can be treated as an unknown in the system of equations by solving combinations of (17)–(21). The solution of these equations is then independent of reference plane position, air line length, and sample length. For example, (20) and (21) constitute four real equations that are independent of reference plane; they can be solved as a system with both the sample length and the air line length treated as unknown quantities.

Another interesting result can be obtained if we assume that ϵ_R^* and the measured value of an S parameter are known at a single angular frequency, ω_k. In this case we can solve either (11) or (12) for the reference positions and then substitute this length into (8)–(10) to obtain relations for the reference plane positions at other fre-

quencies. This length is the equivalent electrical length of the section of line. If we let m denote "measured value" and S denote the right side of either (8) or (10), with $R_1 = R_2 = 1$, we obtain a relation for the reference plane rotation term at an angular frequency of ω_i (for coaxial line):

$$R_1^2(\omega_i) = [S_{11}(\omega_k)]^{(\omega_i/\omega_k)}\left[\frac{1-z^2\Gamma^2}{\Gamma(1-z^2)}\right]^{(\omega_i/\omega_k)} \tag{22}$$

$$R_1(\omega_i)R_2(\omega_i) = [S_{21}(\omega_k)]^{(\omega_i/\omega_k)}\left[\frac{1-z^2\Gamma^2}{z(1-\Gamma^2)}\right]^{(\omega_i/\omega_k)}. \tag{23}$$

Thus, we can determine the reference plane positions in terms of $\epsilon_R^*(\omega_k)$ and the measured value of the scattering parameter at ω_k. Equations (22) and (23) may be very useful for problems where other methods have produced an accurate measurement of ϵ_R^* at a single frequency.

Equations for Numerical Permittivity Determination

There are various ways of solving the scattering equations depending on the information available to the experimenter. For cases where the sample length and reference plane positions are known to high accuracy, we have found that taking various linear combinations of the scattering equations and solving the equations in an iterative fashion yields a very stable solution on samples of arbitrary length. A useful combination is

$$\frac{1}{2}\{[S_{12}+S_{21}]+\beta[S_{11}+S_{22}]\} = \frac{z(1-\Gamma^2)+\beta\Gamma(1-z^2)}{1-z^2\Gamma^2}. \tag{24}$$

In this equation the S parameters to be used need to be transformed from the calibration plane to the sample face by use of (11) and (12). Here β is a constant which we vary as a function of the sample length, uncertainty in scattering parameters, and loss characteristics of the material. For low-loss materials, the S_{21} signal is strong and so we can set β equal to zero, whereas for materials of high loss S_{11} dominates and a large value of β is appropriate. A general relation for β is given by the ratio of the uncertainty in S_{21} divided by the uncertainty in S_{11}. In Fig. 2 the iterative solution (in the dashed line) is compared to the Nicolson–Ross–Weir procedure for a sample of polytetrafluoroethylene (PTFE) in 7 mm coaxial line. We see a striking contrast between the solutions. In Fig. 3 we reduce data for the permittivity for PTFE while varying the parameter β, which has low loss and relatively low ϵ_R'; the best results are produced by using only S_{21} and S_{12} data. One requirement for an iterative technique is the selection of the initial guess for the permittivity. As an initial guess we use the solutions to the Nicolson and Ross equations as a starting value and then use the previously obtained permittivity at one frequency as the initial guess for the next frequency.

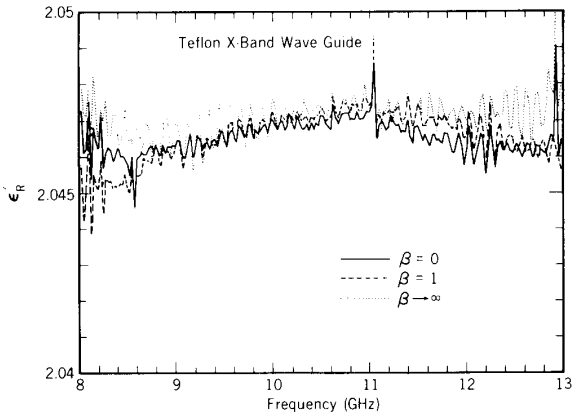

Fig. 3. The permittivities obtained from (24) for various values of β for a sample of PTFE. The dashed line is for $\beta \to \infty$, the solid line for $\beta = 0$, and the dotted line for $\beta = 1$.

For cases in which the reference plane positions are uncertain, we find that (21) is robust. When using (21) no reference plane transformation need be performed since it has been eliminated by use of the relation $L_{\text{air}} = L_1 + L_2 + L$. Equation (21) works well for both low-loss and high-loss materials. If we solve (21) in tandem with any of (17)–(20), we can treat the measurement as independent of reference plane position and sample length.

For magnetic materials, four independent real equations are required (or two independent complex equations). Since in this case we have seven unknowns and nine equations, it is possible to use various combinations of the basic equations (17)–(21); in this case (20) and (21) are recommended. However, for combined permeability and permittivity these equations may not be stable at multiples of one-half wavelength in the sample. To maintain stability another approach is required and results of research will be reported in the near future.

III. Uncertainty Analysis

The sources of error in TR measurement include

- errors in measuring the magnitude and phase of the scattering parameters,
- gaps between the sample and sample holder and sample holder dimensional variations and errors in gap correction formulas,
- uncertainty in sample length,
- line losses and connector mismatch,
- uncertainty in reference plane positions,
- coupling to higher order modes.

The error arising from gaps around the sample can be corrected for in part by using equations available in the literature [12]–[14]. The formulas given in the literature generally undercorrect for the real part of the permittivity and overcorrect for the imaginary part of the permittivity. We assume in the following analysis that all measurements of permittivity have been corrected for air gaps

around the sample before the following uncertainty analysis is applied. Errors from precision air line dimensional variations have been studied by Hill [15] and it was shown that these uncertainties are generally much smaller than the systematic uncertainty introduced by the network analyzer. In order to evaluate the uncertainty introduced by the measured scattering parameters, a differential uncertainty analysis is applicable, with the uncertainty due to S_{11} and S_{21} evaluated separately. We assume that the total uncertainty can be written as

$$\frac{\Delta\epsilon_R'}{\epsilon_R'} = \frac{1}{\epsilon_R'}\sqrt{\left(\frac{\partial\epsilon_R'}{\partial|S_\alpha|}\Delta|S_\alpha|\right)^2 + \left(\frac{\partial\epsilon_R'}{\partial\theta_\alpha}\Delta\theta_\alpha\right)^2 + \left(\frac{\partial\epsilon_R'}{\partial L}\Delta L\right)^2} \tag{25}$$

$$\frac{\Delta\epsilon_R''}{\epsilon_R''} = \frac{1}{\epsilon_R''}\sqrt{\left(\frac{\partial\epsilon_R''}{\partial|S_\alpha|}\Delta|S_\alpha|\right)^2 + \left(\frac{\partial\epsilon_R''}{\partial\theta_\alpha}\Delta\theta_\alpha\right)^2 + \left(\frac{\partial\epsilon_R''}{\partial L}\Delta L\right)^2} \tag{26}$$

where $\alpha = 11$ or 21, $\Delta\theta$ is the uncertainty in the phase of the scattering parameter, $\Delta|S_\alpha|$ is the uncertainty in the magnitude of the scattering parameter, and ΔL is the uncertainty in the sample length. The calculated, $\Delta\epsilon_R^*$, is a worst case estimate. The uncertainty analysis in this section is for the scattering equations in (8)–(10). The derivatives of (8)–(10) can be explicitly calculated. These are given below, assuming $\mu_R^* = 1$:

$$\frac{\partial\epsilon_R^*}{\partial|S_{21}|} = \frac{[1-\Gamma^2z^2]\exp(j\theta)}{Q} \tag{27}$$

$$\frac{\partial\epsilon_R^*}{\partial\theta_{21}} = j|S_{21}|\frac{\partial\epsilon_R^*}{\partial|S_{21}|} \tag{28}$$

$$\left(\frac{\partial\epsilon_R^*}{\partial L}\right)_{S_{21}} = -C\frac{[(1-\Gamma^2)+2S_{21}\Gamma^2z]}{Q} \tag{29}$$

where

$$Q = 2A\Gamma z[S_{21}z-1] + B[(1-\Gamma^2)+2S_{21}\Gamma^2z] \tag{30}$$

$$A = \frac{\omega^2}{2\gamma\gamma_0c_{\text{vac}}^2}\frac{1}{\left(1+\dfrac{\gamma}{\gamma_0}\right)}\left[1+\frac{1-\dfrac{\gamma}{\gamma_0}}{1+\dfrac{\gamma}{\gamma_0}}\right] \tag{31}$$

$$B = \frac{L\omega^2z}{2c_{\text{vac}}^2\gamma} \tag{32}$$

$$C = -\gamma z \tag{33}$$

$$\frac{\partial\epsilon_R^*}{\partial|S_{11}|} = \frac{[1-\Gamma^2z^2]}{P}\exp(j\theta) \tag{34}$$

$$\frac{\partial\epsilon_R^*}{\partial\theta_{11}} = j|S_{11}|\frac{\partial\epsilon_R^*}{\partial|S_{11}|} \tag{35}$$

$$\left(\frac{\partial\epsilon_R^*}{\partial L}\right)_{S_{11}} = \frac{2Cz\Gamma[1-S_{11}\Gamma]}{P} \tag{36}$$

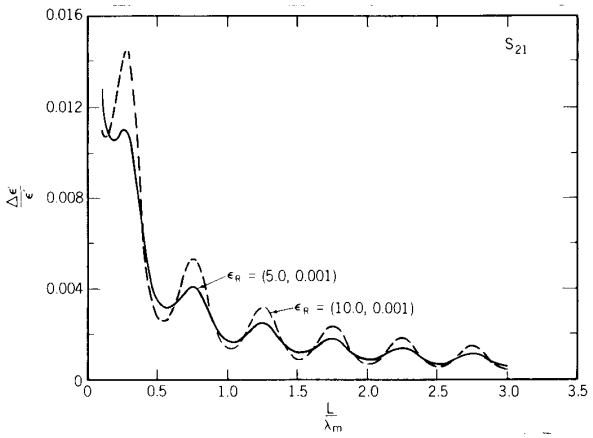

Fig. 4. The relative uncertainty in $\epsilon_R'(\omega)$ for S_{21} from (25) for a low-loss material as a function of normalized length, with $\epsilon_R^* = (5.0, 0.001)$ in solid line and (10.0, 0.001) in dashed line. The uncertainties for the S parameters are those furnished by Hewlett Packard for the 8510B network analyzer.[1]

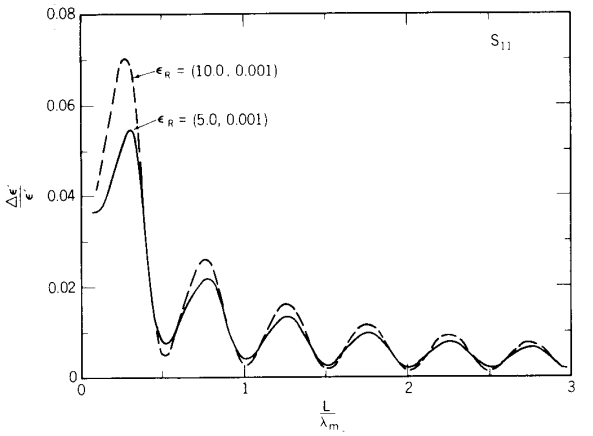

Fig. 5. The relative uncertainty in $\epsilon_R^*(\omega)$ for S_{11} from (25) for a low-loss material as a function of normalized length, with $\epsilon_R^* = (5.0, 0.001)$ in solid line and (10.0, 0.001) in dashed line. The S-parameter uncertainties are the same as in Fig. 4. (See footnote 1.)

where

$$P = A[(1-z^2)+2S_{11}z^2\Gamma] + 2B\Gamma z[S_{11}\Gamma - 1]. \tag{37}$$

The measurement bounds for S-parameter data are obtained from specifications for a network analyzer. The dominant uncertainty is in the phase of S_{11} as $|S_{11}| \to 0$. The uncertainty in $|S_{21}|$ is relatively constant until $|S_{21}| \leq -40$ dB; it then increases abruptly. In Figs. 4–9 the total uncertainty in $\epsilon_R', \epsilon_R''$, calculated from S_{21} and S_{11} is plotted as a function of normalized sample length for coaxial low-loss and high-loss materials at 3 GHz with various values of ϵ_R^* and the guided wavelength in the

[1]Trade names are included in order to allow the reader to duplicate the S-parameter uncertainties. Inclusion does not imply endorsement by the National Institute of Standards and Technology.

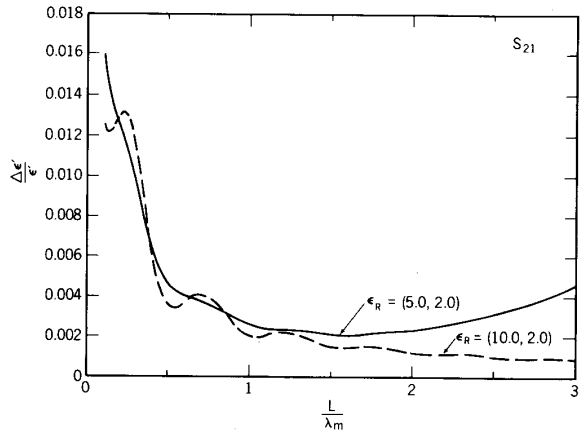

Fig. 6. The relative uncertainty in $\epsilon_R'(\omega)$ for S_{21} from (25) as a function of frequency for a high-loss material as a function of normalized length, with $\epsilon_R^* = (5.0, 2.0)$ in solid line and (10.0, 2.0) in dashed line. The S-parameter uncertainties are the same as in Fig. 4. (See footnote 1.)

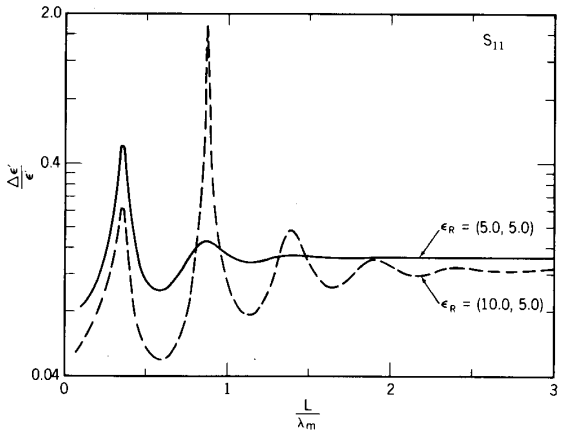

Fig. 8. The relative uncertainty in $\epsilon_R'(\omega)$ for S_{11} (25) as a function of frequency for a high-loss material as a function of normalized length with $\epsilon_R^* = (5.0, 5.0)$ in solid line and (10.0, 5.0) in dashed line. The S-parameter uncertainties are the same as in Fig. 4. (See footnote 1.)

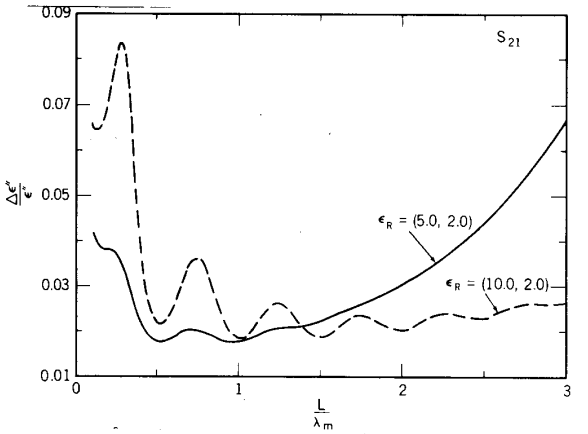

Fig. 7. The relative uncertainty in $\epsilon_R''(\omega)$ for S_{21} from (26) as a function of frequency for a high-loss material as a function of normalized length, for $\epsilon_R^* = (5.0, 2.0)$ in solid line and (10.0, 2.0) in dashed line. The S-parameter uncertainties are the same as in Fig. 4. (See footnote 1.)

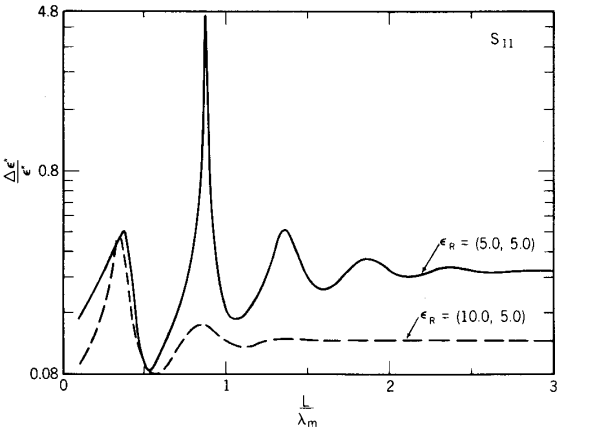

Fig. 9. The relative uncertainty in $\epsilon_R''(\omega)$ for S_{11} from (26) as a function of frequency for a high-loss material as a function of normalized length with $\epsilon_R^* = (5.0, 5.0)$ in solid line and (10.0, 5.0) in dashed line. The S-parameter uncertainties are the same as in Fig. 4. (See footnote 1.)

material given by

$$\lambda_m = \frac{2\pi}{\sqrt{\omega^2 \frac{\left(\sqrt{\epsilon'^2 + \epsilon''^2} + \epsilon'\right)}{2}\mu' - \left(\frac{2\pi}{\lambda_c}\right)^2}}. \quad (38)$$

We see that the minimum uncertainty for low-loss materials occurs at multiples of one-half wavelength. The reason for this can be determined from examination of (8) and (10) in the limit where $|S_{11}| \to 0$, $|S_{21}| \to 1$ with $\Gamma \neq 0$. These equations then reduce to

$$z^2 - 1 \to 0. \quad (39)$$

Generally, we see a decrease in uncertainty as a function of increasing sample length. In the case of S_{21} for high loss as shown in Figs. 6 and 7, we see first a general decrease in uncertainty and then an increase in uncertainty. This increase occurs because $\Delta|S_{21}|$ increases when the transmitted signal is less than -40 dB from the reference. For the case of high loss, the uncertainty in S_{11} approaches a constant value. This is so because, for high-loss materials where the wavelength is much smaller than the sample length, only weak signals penetrate through the sample and thus the front face reflection dominates the S_{11} parameter. In Figs. 8 and 9 we note a number of peaks. These peaks occur when (37) gets very small. Also, the uncertainties in the S parameters have some frequency dependence, with higher frequencies having larger uncertainties in phase. In Fig. 10 a measurement of heavy metal fluoride glass is presented with uncertainty bounds. Note that the peaks of uncertainty coincide with the peaks in the measurement noise. Also note that the uncertainties are quite conservative. This is

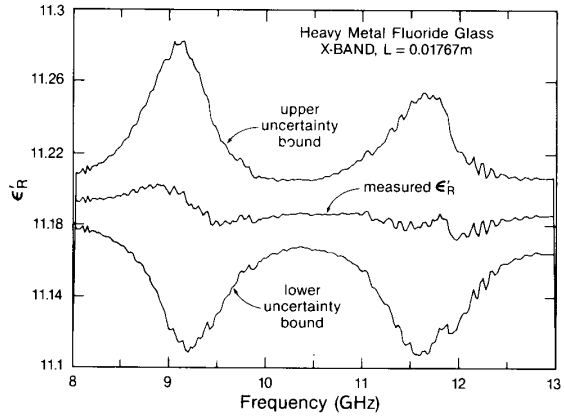

Fig. 10. The permittivity of heavy metal fluoride glass sample in X-band waveguide and calculated uncertainty bounds using (21).

due to the conservative estimate of the manufacturer for the S-parameter uncertainty. When (21) is used for permittivity determination, uncertainties in both S_{21} and S_{11} must be included in (25).

Another important source of error is the uncertainty in the location of the reference planes. Generally, when TR experiments are carried out, the sample is placed flush with the end of the sample holder and hence coincident with a calibration reference plane. This placement procedure leaves room for positioning errors, particularly when the sample is loose. The error introduced by incorrect positioning of the sample can be estimated in terms of the error in the reference plane transformation terms (11) and (12). If we have an uncertainty of ΔL_1 in the sample position, then

$$S_{11} = R_1^2|S_{11}|e^{j\theta} = |S_{11}|\exp\left[j\theta - 2\gamma_0(L_1 + \Delta L_1)\right]. \quad (40)$$

The error in the measured angle is given by

$$\Delta\theta \simeq 2j\gamma_0\Delta L = 4\pi\frac{\Delta L}{\lambda_{\text{air}}}. \quad (41)$$

Therefore small reference plane positioning errors can, in principle, introduce large uncertainties in the S_{11} phase at high frequencies. One way to minimize this is to use equations that are invariant to reference plane position.

IV. Discussion and Conclusions

As we have seen, although the Nicolson–Ross–Weir approach is easy to implement numerically, it fails as a solution technique for broad-band measurement of low-loss samples of arbitrary length. The solution presented in this paper uses a Newton–Raphson iteration procedure on combinations of the scattering parameters. This procedure yields solutions that are stable at integer multiples of one-half wavelength in the sample; at the same time it does not unduly increase the complexity of the numerical solution. For materials where the transmitted signal is more than -40 dB from the reference signal, it is suggested that S_{21} data by themselves are sufficient to calculate permittivity. For materials of large attenuation, S_{11} by itself will produce optimal results. In general, we have found (21) to be robust for high-loss and low-loss materials. The problem of reference plane position has been addressed, and approaches for the minimization of the error have been presented. Equations that are independent of reference plane position and sample length have been presented. Equations that are independent of plane position should be very useful in elevated temperature applications. Generally, sample length can be measured with great accuracy at laboratory temperature, and for these problems it is preferable to use a measured length. However, in temperature-dependent applications it may be better to use equations independent of both sample length and reference plane position.

An uncertainty procedure has been presented for the solution method expounded in this paper. The uncertainty analysis presented here differs in some respects from what has been presented in the literature previously. This difference is due primarily to the fact that the uncertainties in this paper are derived from S_{11} and S_{21} in isolation. The trend indicates that for low-loss materials the uncertainty decreases as a function of increasing sample length. For high-loss materials the uncertainty in S_{21} decreases until the signal reaches -40 to -50 dB, and thereafter the uncertainty increases and thus $\Delta\epsilon_R^*$ increases.

Acknowledgment

The authors wish to thank M. Janezic for help with software development. Dr. R. Geyer, Dr. H. Bussey, and Dr. D. Wait are also thanked for various discussions and for acting as sources of encouragement.

References

[1] A. M. Nicolson and G. F. Ross, "Measurement of the intrinsic properties of materials by time domain techniques," *IEEE Trans. Instrum. Meas.*, vol. IM-17, pp. 395–402, Dec. 1968.

[2] W. W. Weir, "Automatic measurement of complex dielectric constant and permeability at microwave frequencies," *Proc. IEEE*, vol. 62, pp. 33–36, Jan. 1974.

[3] G. A. Deschamps, "Determination of reflection coefficients and insertion loss of a waveguide junction," *J. Appl. Phys.*, vol. 24, no. 8, pp. 1046–1051, Aug. 1953.

[4] Hewlett-Packard. "Measuring dielectric constant with the H.P. 8510 network analyzer." *Hewlett Packard Product note 8510-3.*

[5] M. S. Freeman, R. N. Nottenburg, and J. B. DuBow, "An automated frequency domain technique for dielectric spectroscopy of materials," *J. Phys. E: Sci. Instrum.*, vol. 12, pp. 899–903, 1977.

[6] S. S. Stuchly and M. Matuszewski, "A combined total reflection transmission method in application to dielectric spectroscopy," *IEEE Trans. Instrum. Meas.*, vol. IM-27, pp. 285–288, Sept. 1978.

[7] L. L. Ligthardt, "A fast computational technique for accurate permittivity determination using transmission line methods," *IEEE Trans. Microwave Theory Tech.*, vol. MTT-31, pp. 249–254, Mar. 1983.

[8] H. Altschuler, "Dielectric constant," in *Handbook of Microwave Measurements*, vol. 3, Sucher and Fox, Eds. Brooklyn, NY: Polytechnic Press, 1963, ch. 9, p. 502.

[9] F. J. Harris, "On the use of windows for harmonic analysis with discrete Fourier transform," *Proc. IEEE*, vol. 66, pp. 51–83, Jan. 1978.

[10] W. R. Scott, Jr., and G. S. Smith, "Dielectric spectroscopy using monopole antennas of general electrical length," *IEEE Trans. Antennas Propagat.*, vol. AP-35, pp. 962–967, Aug. 1987.

[11] D. M. Kerns and R. W. Beatty, *Basic Theory of Waveguide Junctions and Introductory Microwave Network Analysis*. New York: Pergamon Press, 1967.
[12] W. P. Westphal, "Techniques of measuring the permittivity and permeability of liquids and solids in the frequency range 3 c/s to 50 kmc/s," Tech. Rep. XXXVI, Laboratory for Insulation Research, Massachusetts Institute of Technology, pp. 99–104, 1950.
[13] H. Bussey, "Measurements of RF properties of materials: A survey," *Proc. IEEE*, vol. 55, pp. 1046–1053, June 1967.
[14] H. E. Bussey and J. E. Gray, "Measurement and standardization of dielectric samples," *IRE Trans. Instrum.*, vol. I-11, no. 3, pp. 162–165, 1962.
[15] D. A. Hill, "Reflection coefficient of a waveguide with slightly uneven walls," *IEEE Trans. Microwave Theory Tech.*, vol. 37, pp. 244–252, Jan. 1989.

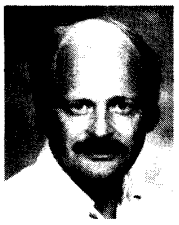

James Baker-Jarvis (M'89) was born in Minneapolis, MN, and received the B.S. degree in 1975 in mathematics. He then spent a year as a research assistant in the University of Minnesota Space Sciences Center working on a NASA grant investigating magnetic properties of lunar rock samples, and two years at the Mineral Resources Research Center at the University of Minnesota. He received the master's degree in physics in 1980 from the University of Minnesota and the Ph.D. in physics in 1984 from the University of Wyoming.

He worked as an AWU postdoctoral fellow for one year on theoretical and experimental aspects of intense electromagnetic fields in lossy materials. He then spent two and a half years as a temporary assistant professor in the Physics Department at the University of Wyoming, where in addition to being coleader of a group on electromagnetic heating of fossil fuels, he taught and performed research on electromagnetic propagation in lossy materials. From then until 1988 he was Assistant Professor of Physics at North Dakota State University. He has recently developed a number of innovative techniques to solve differential equations using maximum entropy techniques. He joined the National Institute of Standards and Technology in January 1989, where his interests are in the areas of dielectric properties and measurements and nondestructive evaluation.

Dr. Baker-Jarvis is the author of numerous publications in such areas as electromagnetics, kinetic theory of fracture, hydrodynamics, heat transfer, maximum entropy methods, and numerical simulation. He also has been principal investigator on a number of research grants. He is a member of APS, the American Association of Physics Teachers, and Sigma Xi.

Eric J. Vanzura (M'90) was born in Pasadena, TX, and grew up in Albuquerque, NM. He graduated from the University of Colorado in Boulder in 1984 with the B.S. degree in engineering physics.

Since joining the National Bureau of Standards (now the National Institute of Standards and Technology, (NIST)) in 1982, he has authored or coauthored four papers and has worked on projects which include the generation and characterization of electromagnetic fields in the 50 to 200 MHz band, the measurement of conducted electromagnetic interference (CEMI), the development of standardized methods for measuring the shielding effectiveness of materials, and the development of measurement techniques for determining dielectric properties at microwave and millimeter-wave frequencies.

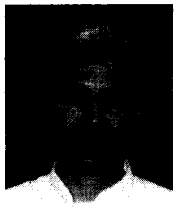

William A. Kissick (M'88) was born in Kittanning, PA. He attended the Pennsylvania State University and received the B.S. degree in electrical engineering in 1969. In the same year he joined the Ionosphere Research Laboratory at Penn State to study ground-based radio measurements of the ionosphere. He received the M.S. and Ph.D. degrees in electrical engineering in 1970 and 1974, respectively.

He began working for the U.S. government in Boulder, CO, when he joined the Institute for Telecommunications Sciences (ITS) in 1975. Until 1983, as Project Leader, he developed and applied models of terrestrial radio wave propagation and conducted a number of field measurements. From 1984 to 1987 he was Chief of the Advanced Networks Analysis Group at ITS, where he developed programs to study the performance of radio, wire, fiber-optic, satellite, and mixed-media telecommunications networks. In 1987 he joined the Electromagnetic Fields Division of the National Bureau of Standards (now the National Institute of Standards and Technology (NIST)), where his current interests are dielectric and magnetic materials and microwave and millimeter-wave metrology. He is currently Leader of the Broadband Microwave Metrology Group in the Electromagnetic Fields Division at NIST.

Dr. Kissick is a member of the IEEE Microwave Theory and Techniques Society, Eta Kappa Nu, Sigma Tau, Phi Kappa Phi, and Tau Beta Pi.